bioRxiv preprint doi: https://doi.org/10.1101/2023.09.25.559286; this version posted September 25, 2023. The copyright holder for this preprint (which was not certified by peer review) is the author/funder, who has granted bioRxiv a license to display the preprint in perpetuity. It is made available under aCC-BY-ND 4.0 International license.

CDK8/19 Inhibition Attenuates G1 Arrest Induced by BCR-ABL Antagonists and Accelerates Death of Chronic Myelogenous Leukemia Cells

Alvina I. Khamidullina[1,2], Margarita A. Yastrebova[1,2], Alexandra V. Bruter[2], Julia V. Nuzhina[1,2], Nadezhda E. Vorobyeva[1], Anastasia M. Khrustaleva[1], Ekaterina A. Varlamova[2], Alexander V. Tyakht[1,2], Yaroslav E. Abramenko[1], Ekaterina S. Ivanova[3], Maria A. Zamkova[1,3], Jing Li[4], Chang-Uk Lim[4], Mengqian Chen[4,5], Eugenia V. Broude[4], Igor B. Roninson[4], Alexander A. Shtil[1,3], and Victor V. Tatarskiy[1]*

[1]Institute of Gene Biology, Russian Academy of Sciences, 34/5 Vavilov Street, 119334 Moscow, Russia

[2]Center for Precision Genome Editing and Genetic Technologies for Biomedicine, Institute of Gene Biology, Russian Academy of Sciences, 34/5 Vavilov Street, 119334 Moscow, Russia

[3]Blokhin National Medical Research Center of Oncology, 24 Kashirskoye shosse, 115522 Moscow, Russia

[4]Department of Drug Discovery and Biomedical Sciences, University of South Carolina, 715 Sumter Street, Columbia, SC 29208, USA

[5]Senex Biotechnology, Inc., 715 Sumter Street, Columbia, SC 29208, USA

*Corresponding author: tatarskii@gmail.com

Scopus Author ID: 9637507400

ResearcherID: K-1224-2017

ORCID ID 0000-0002-9080-5683

bioRxiv preprint doi: https://doi.org/10.1101/2023.09.25.559286; this version posted September 25, 2023. The copyright holder for this preprint (which was not certified by peer review) is the author/funder, who has granted bioRxiv a license to display the preprint in perpetuity. It is made available under aCC-BY-ND 4.0 International license.

Abstract

Imatinib and other selective inhibitors of BCR-ABL are the mainstay of chronic myelogenous leukemia (CML) treatment, but resistance to these drugs limits their efficacy. Known resistance mechanisms include *ABL* mutations, activation of compensatory signaling pathways, and the induction of quiescence that protects CML cells from apoptosis. CDK8/19 Mediator kinases that regulate transcriptional reprogramming have been implicated in the development of resistance to different drugs. We have investigated the effects of CDK8/19 inhibition on CML response to BCR-ABL inhibitors. Selective CDK8/19 inhibitors Senexin B and SNX631 strongly increased the induction of apoptosis in K562 cells treated with imatinib or other BCR-ABL inhibitors. Imatinib induced G1 arrest along with upregulation of $p27^{Kip1}$, but these effects were suppressed by CDK8/19 inhibition. Senexin B also prevented the induction of G1 arrest and protection from imatinib-induced apoptosis of K562 cells by inducible $p27^{Kip1}$ expression, suggesting that CDK8/19 activity potentiates both the transcription and function of $p27^{Kip1}$. In contrast, CDK8/18 inhibition did not have the same effect in KU812 CML cells that do not undergo G1 arrest and are hypersensitive to imatinib. Our results suggest that inhibition of CDK8/19 may be used as a new strategy to prevent quiescence-mediated resistance to BCR-ABL inhibitors.

Key words

CDK8/19; BCR-ABL; imatinib; chronic myelogenous leukemia; cell death.

List of abbreviations

BCR-ABLi, BCR-ABL inhibitor(s);

CDK, cyclin-dependent kinase;

CDK8/19i, CDK8/19 inhibitor(s);

CKI, cyclin-dependent kinase inhibitor;

CML, chronic myelogenous leukemia;

Das, dasatinib;

DEG, differentially expressed genes;

Dox, doxycycline;

IM, imatinib mesylate;

LSC, leukemia stem cells;

Nilo, nilotinib;

PARP, poly (ADP-ribose) polymerase;

SenB, senexin B.

bioRxiv preprint doi: https://doi.org/10.1101/2023.09.25.559286; this version posted September 25, 2023. The copyright holder for this preprint (which was not certified by peer review) is the author/funder, who has granted bioRxiv a license to display the preprint in perpetuity. It is made available under aCC-BY-ND 4.0 International license.

Introduction

Chronic myelogenous leukemia (CML) is a myeloproliferative disorder characterized by an expansion of pluripotent bone marrow stem cells. The main genetic marker of CML is the Philadelphia chromosome generated by translocation t(9;22)(q34;q11). This translocation yields the BCR-ABL chimeric tyrosine kinase, which activates a number of downstream pathways that drive the pathogenesis of CML as well as a minor subset of other leukemias (1).

Introduction of the tyrosine kinase inhibitor imatinib mesylate (IM, Gleevec) has drastically improved CML treatment outcomes (2). However, a significant proportion of patients eventually develop resistance to BCR-ABL antagonists that can be attributed to *BCR-ABL* mutations or independent signaling pathways (3). Second generation BCR-ABL inhibitors (BCR-ABLi) such as nilotinib, dasatinib and bosutinib, are used for treatment of patients with certain mutations in *BCR-ABL* but are inefficient against the T315I mutation. While the third generation BCR-ABLi ponatinib, asciminib and PF-114 are effective against specific *BCR-ABL* mutants including T315I, these drugs are limited in their ability to circumvent BCR-ABL-independent drug resistance (4).

BCR-ABL-independent resistance is mediated by signaling pathways that involve STAT3 (5,6), MAPK/ERK (7), β-catenin (8). One of the most refractory populations are the dormant leukemia stem cells (LSC) capable of prolonged persistence (9). In CML, quiescence is a mechanism that can prevent the achievement of full clinical remission (10). Moreover, quiescent CML cells may reenter the cell cycle, leading to a relapse (11). Cell cycle arrest and quiescence are regulated by cyclin dependent kinase inhibitor (CKI) proteins of CIP/KIP ($p27^{Kip1}$, $p57^{Kip2}$, and $p21^{Cip1}$) and INK4 ($p18^{INC4c}$ and other) families (12,13). BCR-ABL abrogates the $p27^{Kip1}$ function (14–17), and inhibition of BCR-ABL by IM induces $p57^{Kip2}$ followed by overexpression and stabilization of $p27^{Kip1}$ (18). These data indicate that CML resistance to BCR-ABL inhibitors is associated with cell cycle arrest and quiescence can be regulated epigenetically. Indeed, pharmacological intervention into the mechanisms of epigenetic modulation has been shown to be beneficial for exit from quiescence, therefore increasing tumor cell death (19).

The cyclin dependent kinase 8 (CDK8) or its paralog CDK19, together with cyclin C (CCNC), MED12, and MED13, form a module that binds to the transcriptional Mediator complex (20). The Mediator kinase module regulates transcription by tuning the transcriptional machinery via the Mediator and transcription factor function at enhancers and promoters. Also, the CDK module acts as a modifier of different cancer-relevant transcription factors and coordinates the response to exogenous stimuli by reprogramming gene expression (21). While CDK8/19 potentiate the induction of transcription by several different signals, they also inhibit Mediator-dependent transcription of super-enhancer-associated genes (22), in conjunction with post-transcriptional downregulation of the Mediator complex (23). CDK8/19 modulate transcription factors such as STATs (24), NF-κB (25), and others. Importantly, CDK8 depletion does not affect viability in the adult cells or organisms, making these enzymes attractive drug targets (26,27).

The role of CDK8/19-mediated transcriptional reprogramming in acquired drug resistance was demonstrated by the ability of small-molecule CDK8/19 inhibitors (CDK8/19i) to sensitize tumor cells or to prevent the emergence of resistance to chemotherapeutics including inhibitors of estrogen receptor and EGFRs (28–30). Thus, CDK8/19i are considered as antitumor drug candidates in combined regimens. Several CDK8/19i have reached clinical trials in solid tumors and leukemias (NCT03065010, NCT04021368, NCT05052255, NCT05300438).

bioRxiv preprint doi: https://doi.org/10.1101/2023.09.25.559286; this version posted September 25, 2023. The copyright holder for this preprint (which was not certified by peer review) is the author/funder, who has granted bioRxiv a license to display the preprint in perpetuity. It is made available under aCC-BY-ND 4.0 International license.

Here, we present evidence that CDK8/19i inhibit the induction of cell cycle arrest by BCR-ABLi mediated by cell cycle inhibitor $p27^{Kip1}$ in CML cells, greatly potentiating the induction of apoptosis. These results suggest that inhibition of CDK8/19 may prevent quiescence-mediated resistance to BCR-ABL inhibitors.

Results

Senexin B synergizes with IM in triggering apoptosis in K562 cells

We tested whether a selective CDK8/19 inhibitor Senexin B (SenB) (28,29,43) affects CML cell response to BCR-ABL antagonist IM. Figure 1A, *left* shows that SenB sensitized K562 cells to IM. By 72 h the percentage of viable cells was larger in the IM-treated cohort than in the combination. The portion of PI-positive (late apoptosis) cells greatly increased in the combination: from 15.0±0.3% in cells treated with IM alone to 54.0±0.6% in the combination of IM and SenB (Figure 1A, *right*; $p<0.0001$). The time course showed that, already by 24 h, 1 μM SenB strongly increased the percentage of subG1 events (cells with fragmented DNA) after treatment with low concentrations of IM (Figure 1B, *left*; compare 11.6±2.2% in cells treated with 0.25 μM IM *vs* 24.6±1.4% after 0.25 μM IM and 1 μM SenB ($p<0.0001$)). Potentiation of the induction of apoptosis was detectable even with submicromolar concentrations of SenB (Figure 1B, *right*). SenB alone did not increase the percentage of double positive Annexin V^+/PI^+ cells but synergized with IM in elevating this fraction by 24 h (Figure 1C, *top*, Supplementary Figure S1). As opposed to K562 cells, the BCR-ABL positive KU812 CML cell line was intrinsically hypersensitive to IM-induced apoptosis, and the addition of SenB had no significant effect on the already very high apoptotic fraction (Figure 1C, *bottom*, Supplementary Figure S1).

bioRxiv preprint doi: https://doi.org/10.1101/2023.09.25.559286; this version posted September 25, 2023. The copyright holder for this preprint (which was not certified by peer review) is the author/funder, who has granted bioRxiv a license to display the preprint in perpetuity. It is made available under aCC-BY-ND 4.0 International license.

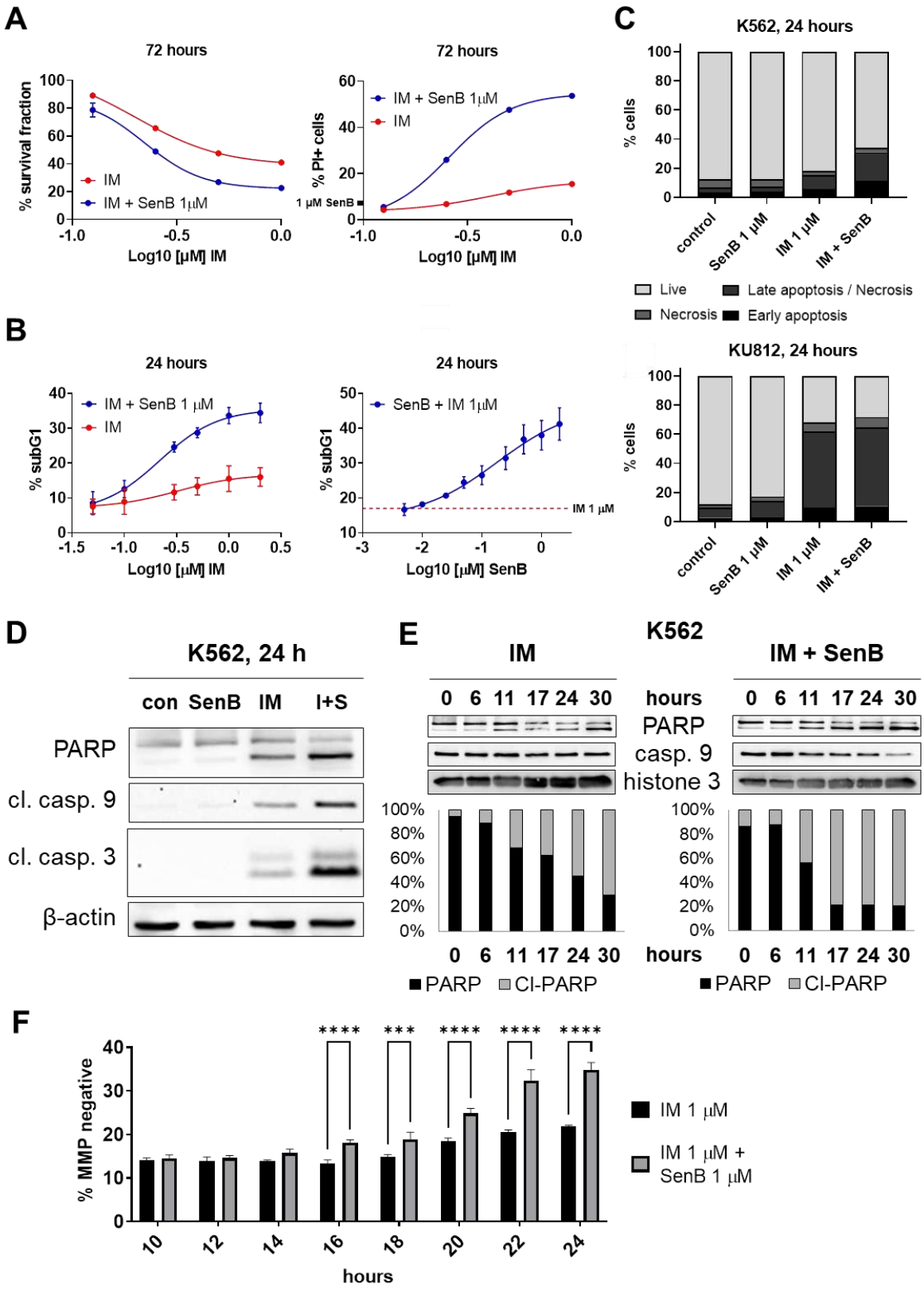

Figure 1. SenB synergizes with IM in inducing K562 apoptosis. Cells were treated with SenB, IM (1 μM each) or their combination (I+S) for indicated time periods, stained with PI (**A**), lysed in the PI containing buffer (**B),** stained with Annexin V-PI (**C**) and analyzed by flow cytometry. **C**: *Top*, K562; *bottom*, KU812. Values are mean±SD, n=4. (**D**) Immunoblotting of PARP, cleaved caspases 9 and 3 and β-actin (control) after 24 h. (**E**) Time course of PARP cleavage and caspase 9 activation. *Top*, gel images; *bottom*, densitometry data. (**F**) Time course of the loss of the mitochondrial membrane potential (MMP). ***p<0.001, ****p<0.0001.

bioRxiv preprint doi: https://doi.org/10.1101/2023.09.25.559286; this version posted September 25, 2023. The copyright holder for this preprint (which was not certified by peer review) is the author/funder, who has granted bioRxiv a license to display the preprint in perpetuity. It is made available under aCC-BY-ND 4.0 International license.

Next, we found that the combined inhibition of CDK8/19 and BCR-ABL increased the activation of caspases 9 and 3 and cleavage of poly(ADPriboso)polymerase (PARP) in K562 cells, pointing to the mitochondrial apoptosis as a mechanism of sensitization (Figure 1D). Time course (Figure 1E) showed that combination of IM and SenB induced a faster PARP cleavage and decrease of procaspase 9. The addition of SenB significantly increased IM-induced loss of the mitochondrial membrane potential after 16 h (Figure 1F), also indicating that SenB accelerated the onset of IM-induced apoptosis.

SenB potentiated cell death induced not only by IM but also by other BCR-ABL antagonists of different chemical classes and specificity (Figures 2A-B). Furthermore, the synergy with IM was also shown for the second, chemically unrelated CDK8/19i SNX631 (30,44), indicating that the sensitization was a general effect of CDK8/19 inhibition (Figures 2C-D).

The S727 site of STAT transcription factors is a known target of CDK8 that regulates STAT-mediated transcription (24). In the absence of interferon signaling, CDK8/19 inhibition often but not always reduces STAT S727 phosphorylation (43). SenB or IM alone had no significant effect on the amount of pSTAT1 S727 in K562 cells, but this amount was decreased by the combination of IM and SenB (Figure 2E). This decrease was due both to the inhibition of STAT1 S727 phosphorylation and a decrease in total STAT1. Combinational treatment with SenB and IM also reduced pSTAT3 S727 but not total STAT3, indicating the inhibition of STAT3 S727 phosphorylation. STAT3 S727 phosphorylation that augments STAT3 transcriptional activity was shown to be stimulated by BCR-ABL (45) and to play a role in resistance to BCR-ABLi (46).

bioRxiv preprint doi: https://doi.org/10.1101/2023.09.25.559286; this version posted September 25, 2023. The copyright holder for this preprint (which was not certified by peer review) is the author/funder, who has granted bioRxiv a license to display the preprint in perpetuity. It is made available under aCC-BY-ND 4.0 International license.

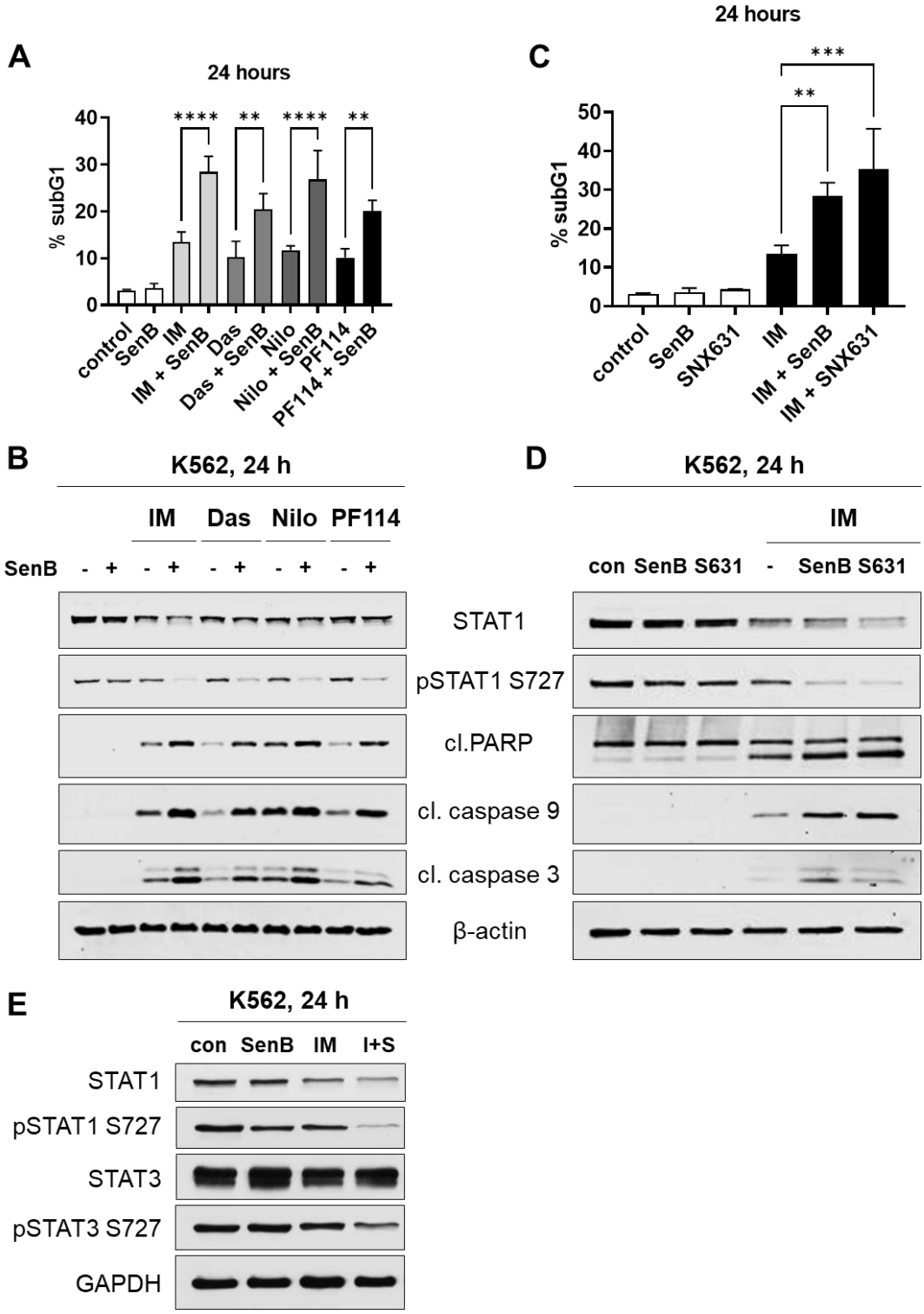

Figure 2. Combinations of CDK8/19 inhibitors and BCR-ABL antagonists cooperatively inhibit STAT1 and STAT3 S727 phosphorylation and induce apoptosis in K562 cells.

K562 cells were treated with SenB, IM (1 μM each) or their combination (I+S) for 24 h. (**A**) Percentages of subG1 events in untreated cells and cells treated by 1 μM IM, 1 nM dasatinib (das), 50 nM nilotinib (nilo) or 10 nM PF114 without or with 1 μM SenB. (**B**) Effects of BCR-ABL inhibitors alone and in combination with SenB on STAT1, pSTAT1 S727 and cleaved PARP, caspase 9 and caspase 3 (immunoblot analysis). Effects of CDK8/19 inhibitors SenB and SNX631 (S631) in combination with IM on subG1 events (**C**) and biochemical markers of cell death (**D**). (**E**) Effects on pSTAT1 S727, STAT3 and pSTAT3 S727. *p<0.05, ***p<0.001, ****p<0.0001.

bioRxiv preprint doi: https://doi.org/10.1101/2023.09.25.559286; this version posted September 25, 2023. The copyright holder for this preprint (which was not certified by peer review) is the author/funder, who has granted bioRxiv a license to display the preprint in perpetuity. It is made available under aCC-BY-ND 4.0 International license.

Effects of IM and SenB on gene expression

RNA sequencing revealed changes in gene expression patterns after 8 h treatment with SenB or IM alone or in combination. Comparisons between the effects of different treatments are shown in the volcano plots in Supplementary Figures S2-S5 and DEG are listed in Supplementary Tables S2-S3. IM induced down-regulation of 2 100 genes, and up-regulation of 1 756 genes, whereas SenB down-regulated 679 genes and up-regulated 1 017 genes (Supplementary Figures S2, S3). Combination of SenB and IM induced down-regulation of 2 394 genes and up-regulation of 2 073 genes (Supplementary Figure S4). The combination changed the expression of 1 185 (down-regulation) and 1 492 mRNAs (up-regulation) compared to IM alone (Supplementary Figure S5). Among the most affected genes that significantly changed in response to IM, 6.1% (163 genes) were differentially expressed between the IM and IM+SenB groups (Figure 3A). Among the genes that were most strongly affected by IM, SenB most often enhanced their upregulation but counteracted their downregulation by IM (Figure 3B). GSEA (39) and ORA (42) showed that many of the genes down-regulated by IM were related to cell proliferation and interferon/STAT signaling (Figures 3C, Supplementary Figure S6), coding for pro-proliferative proteins and individual cell cycle inhibitors. Notably, 17.1 % of all DEG down-regulated in combination compared to IM alone were genes related to the cell cycle, while only 2.1 % were upregulated. The top 5 cell cycle genes downregulated by IM (*VASH1*, *PCBP4*, *GPNMB*, *INHA* and *BTN2A2*) are all related to negative regulation of the cell cycle – induction of cell cycle arrest (Supplementary Figure S7). The addition of SenB produced no major changes in the overall effects of IM on such pathways (Figure 3C), but many of the individual genes that were differentially affected by the combination of IM and Sen B relative to IM alone were associated with cell proliferation (Figure 3D).

bioRxiv preprint doi: https://doi.org/10.1101/2023.09.25.559286; this version posted September 25, 2023. The copyright holder for this preprint (which was not certified by peer review) is the author/funder, who has granted bioRxiv a license to display the preprint in perpetuity. It is made available under aCC-BY-ND 4.0 International license.

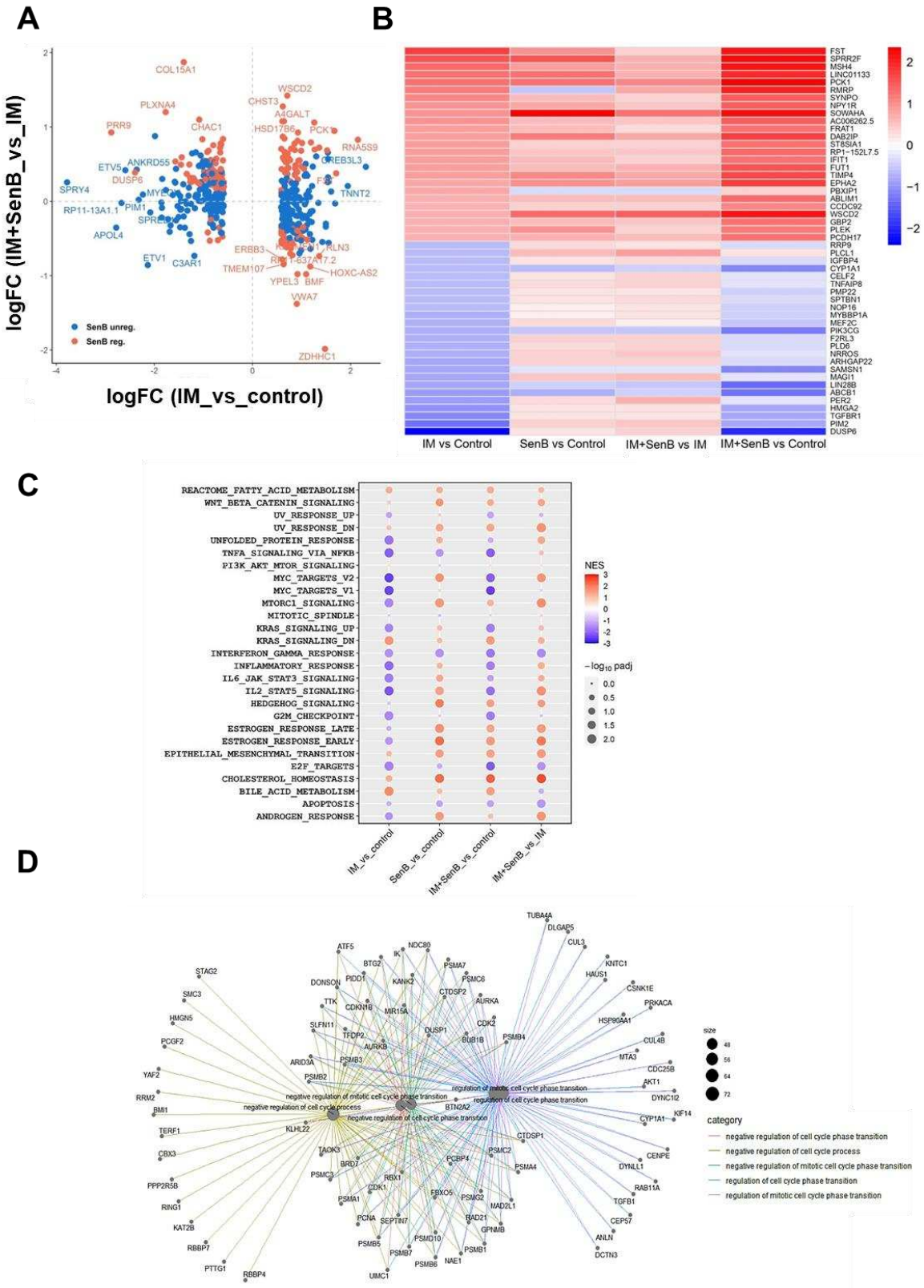

Figure 3. RNA-Seq analysis of K562 cells treated with SenB, IM (1 μM each) and combinations. (**A**) A dot plot comparing the effects of IM *vs* control and IM+SenB *vs* IM on the differentially expressed genes (DEG) affected by IM (|FC|>1.5, FDR<0.01). Red dots – IM DEG regulated by SenB, blue dots – IM DEG unregulated by SenB. (**B**) The heatmap of the effects of different treatments on the genes that are most strongly upregulated or downregulated by IM. Scale is normalized enrichment score (NES). (**C**) Effects of different treatments on the indicated pathways. (**D**) Genes downregulated in SenB+IM-treated cells compared to IM alone.

bioRxiv preprint doi: https://doi.org/10.1101/2023.09.25.559286; this version posted September 25, 2023. The copyright holder for this preprint (which was not certified by peer review) is the author/funder, who has granted bioRxiv a license to display the preprint in perpetuity. It is made available under aCC-BY-ND 4.0 International license.

CDK8/19 inhibition abrogates IM-induced G1 arrest mediated by p27^{Kip1}

According to the results of RNA-Seq analysis, cell proliferation driver *MYC* (c-Myc) was downregulated by IM but upregulated by SenB; *MYC* expression in cells treated with the combination of IM and SenB did not change *MYC* expression relative to the control (Figure 4A, *left*). In contrast, cell cycle inhibitor *CDKN1B* (p27^{Kip1}) was strongly upregulated by IM and downregulated by SenB, and SenB+IM combination did not change *CDKN1B* expression relative to the control (Figure 4A, *right*). p27^{Kip1}, a major mediator of G1 checkpoint, is known to be involved in the response to IM (47,48). Figure 4B shows that IM treatment increases p27^{Kip1} protein in K562 cells in a dose-dependent manner whereas SenB fully prevents this increase. IM also upregulated two other CKIs, p57^{Kip2} and p18^{INC4c}; the increase in p57^{Kip2} was unaffected and in p18^{INC4c} weakly inhibited by SenB (Figure 4C). Similarly, the addition of SenB slightly reduced the effect of IM treatment on the reduction of c-Myc protein (Figure 4C, *left*), an effect paralleled by changes of c-Myc dependent transcripts (Figure 3C).

The dramatic effects of IM on p27^{Kip1}, which was fully suppressed by SenB, suggested that p27^{Kip1}-mediated cell cycle inhibition by IM could play a key role in the prevention of apoptosis, which was counteracted by CDK8/19 inhibition. In agreement with this hypothesis, a very different pattern was observed in KU812 cells that are hypersensitive to IM and unaffected by CDK8/19 inhibition: p27^{Kip1}, p18^{INC4c} and c-Myc were not induced in KU812; instead, disappearance of c-Myc and p21^{Cip1} was detectable already by 7 h of IM treatment and unaffected by SenB (Figure 4C, *right*).

bioRxiv preprint doi: https://doi.org/10.1101/2023.09.25.559286; this version posted September 25, 2023. The copyright holder for this preprint (which was not certified by peer review) is the author/funder, who has granted bioRxiv a license to display the preprint in perpetuity. It is made available under aCC-BY-ND 4.0 International license.

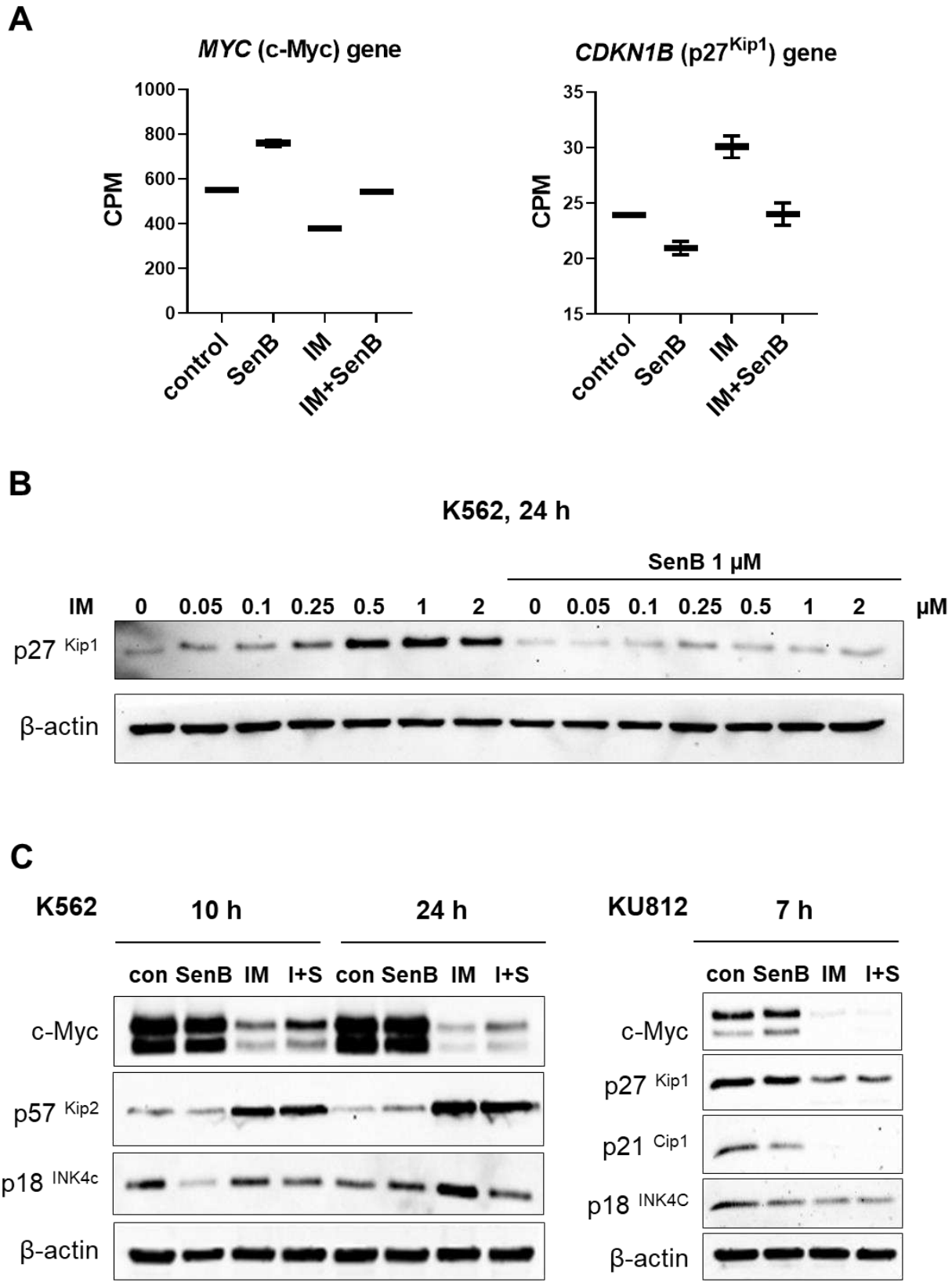

Figure 4. Effects of SenB, IM and their combination on cell cycle regulating genes and proteins. K562 and KU812 cells were treated as indicated. Proteins were analyzed by immunoblotting, mRNAs by RNA-Seq.

(**A**) Abundance of *MYC* (c-Myc) and *CDKN1B* ($p27^{Kip1}$) mRNAs, normalized counts per million (CPM) of reads. (**B**) Effects of IM and SenB on $p27^{Kip1}$ protein. (**C**) Effects of IM and SenB on c-Myc, $p57^{Kip2}$ and $p18^{INC4c}$ protein levels in K562 (*left*) and c-Myc, $p27^{Kip1}$, $p21^{Cip1}$, $p18^{INC4c}$ and caspase 3 cleavage levels in KU812 (*right*), at the indicated time points.

bioRxiv preprint doi: https://doi.org/10.1101/2023.09.25.559286; this version posted September 25, 2023. The copyright holder for this preprint (which was not certified by peer review) is the author/funder, who has granted bioRxiv a license to display the preprint in perpetuity. It is made available under aCC-BY-ND 4.0 International license.

As shown in Figure 5A (*top left*), by 10 h of IM treatment, K562 cells underwent G1 arrest similarly to IM+SenB treated counterparts. However, while G1 arrest caused by IM alone was maintained for the entire 32 h observation period, this arrest was transient in cells treated with a combination of IM and SenB, and subsequently a portion of cells re-entered the cycle. The cell cycle re-entry in combination-treated cells was paralleled by a greater increase in apoptosis relative to cells treated with IM alone (Figure 5A, *bottom left*). These data were substantiated by the increased incorporation of BrdU (Figure 5B) after treatment with SenB+IM. Therefore the combination elevated the fraction of cells that resumed DNA replication. In contrast to K562, the highly IM sensitive KU812 cells did not undergo G1 arrest and readily died (Figure 5A, *right*).

bioRxiv preprint doi: https://doi.org/10.1101/2023.09.25.559286; this version posted September 25, 2023. The copyright holder for this preprint (which was not certified by peer review) is the author/funder, who has granted bioRxiv a license to display the preprint in perpetuity. It is made available under aCC-BY-ND 4.0 International license.

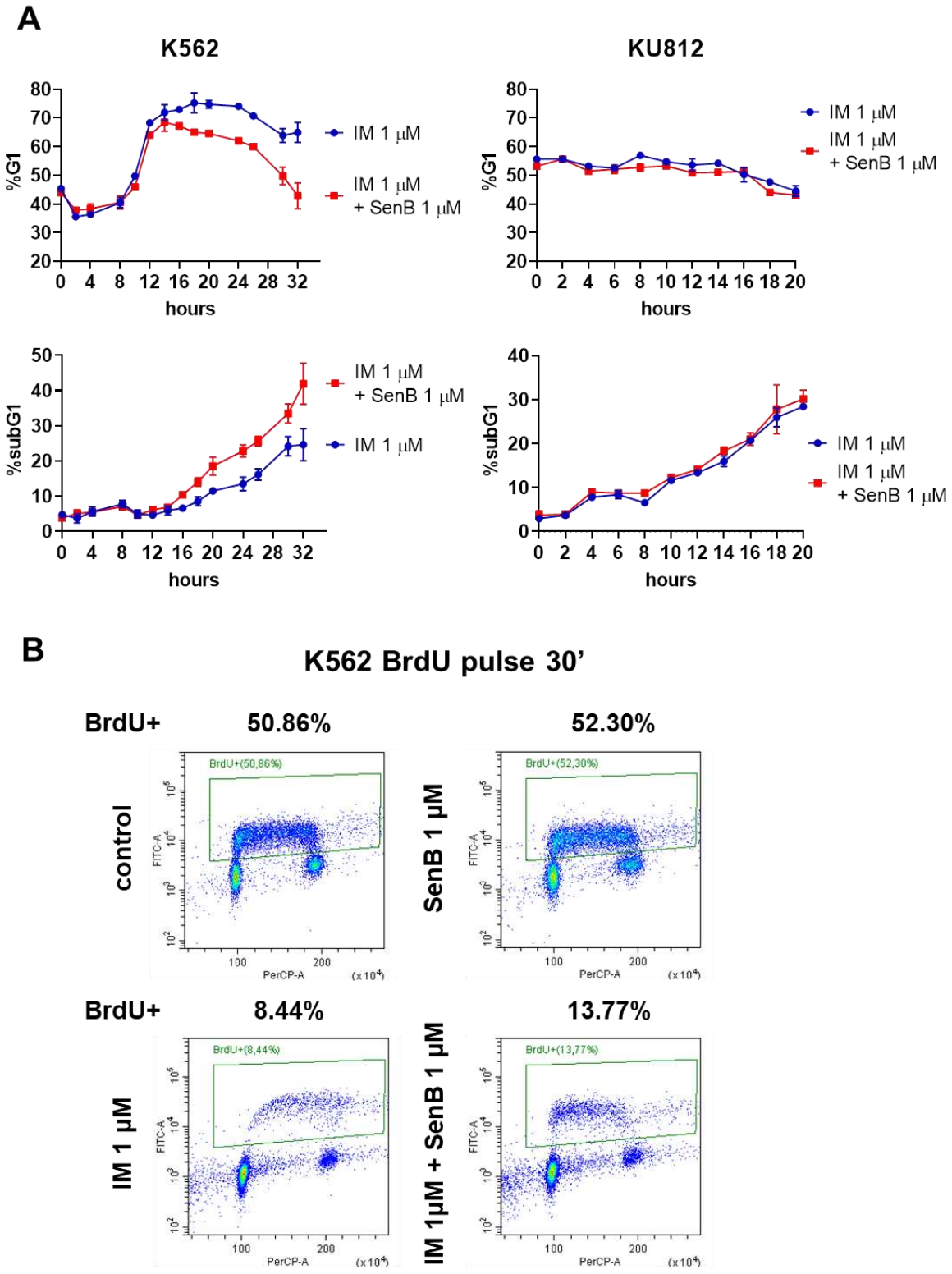

Figure 5. SenB alleviates IM-induced G1 arrest.

(**A**) Time course of G1 and subG1 (apoptotic) fractions of K562 (*left*) and KU812 (*right*) cells treated with IM and SenB (1 μM each). Note that IM alone in K562 caused a sustained accumulation in G1 whereas in the IM+SenB group the portion of cells in G1 gradually decreased (*top left*). Concomitantly, cells treated with the combination died more readily than in the 'IM alone' cohort (*bottom left*). (**B**) K562 cells treated with SenB+IM for 24 h re-entered the cycle more readily (note a larger BrdU positive population) compared to 'IM alone' counterparts (*bottom left vs bottom right*). Shown is one representative experiment out of three biological replicates.

bioRxiv preprint doi: https://doi.org/10.1101/2023.09.25.559286; this version posted September 25, 2023. The copyright holder for this preprint (which was not certified by peer review) is the author/funder, who has granted bioRxiv a license to display the preprint in perpetuity. It is made available under aCC-BY-ND 4.0 International license.

To investigate whether p27^{Kip1} can mediate the sensitization of K562 cells to IM by SenB, we generated the inducible K562p27tet-on derivative in which the exogenous *CDKN1B* is expressed under the control of doxycycline-inducible promoter. Before the addition of doxycycline, the percentage of K562p27tet-on cells in G1 phase was 35.3±1.6%; by 24 h of doxycycline treatment, this value increased up to 64.8±0.7%, p<0.0001. SenB attenuated doxycycline-induced G1 accumulation in a dose dependent manner (Supplementary Figure S8). IM, together with doxycycline, further elevated the G1 fraction, whereas SenB abrogated this increase (Figure 6A, *left*). This effect of SenB was paralleled by the increase of subG1 events (Figure 6A, *right*). As shown in Figure 6B, doxycycline partially prevented IM-induced apoptosis in K562p27tet-on cells: 17.3±2.7% subG1 events in 'no doxycycline' group *vs* 11.6±0.4% in 'doxycycline' cohort, p<0.01. In contrast, the addition of SenB increased the percentage of the subG1 phase to 26.4±3.4% overcoming the protective effect of p27^{Kip1} induction. SenB also partially decreased p27^{Kip1} levels with and without the addition of doxycycline (Figure 6C). These results provide additional evidence that CDK8/19 inhibition sensitized cells to IM via alleviation of p27^{Kip1} associated G1 arrest.

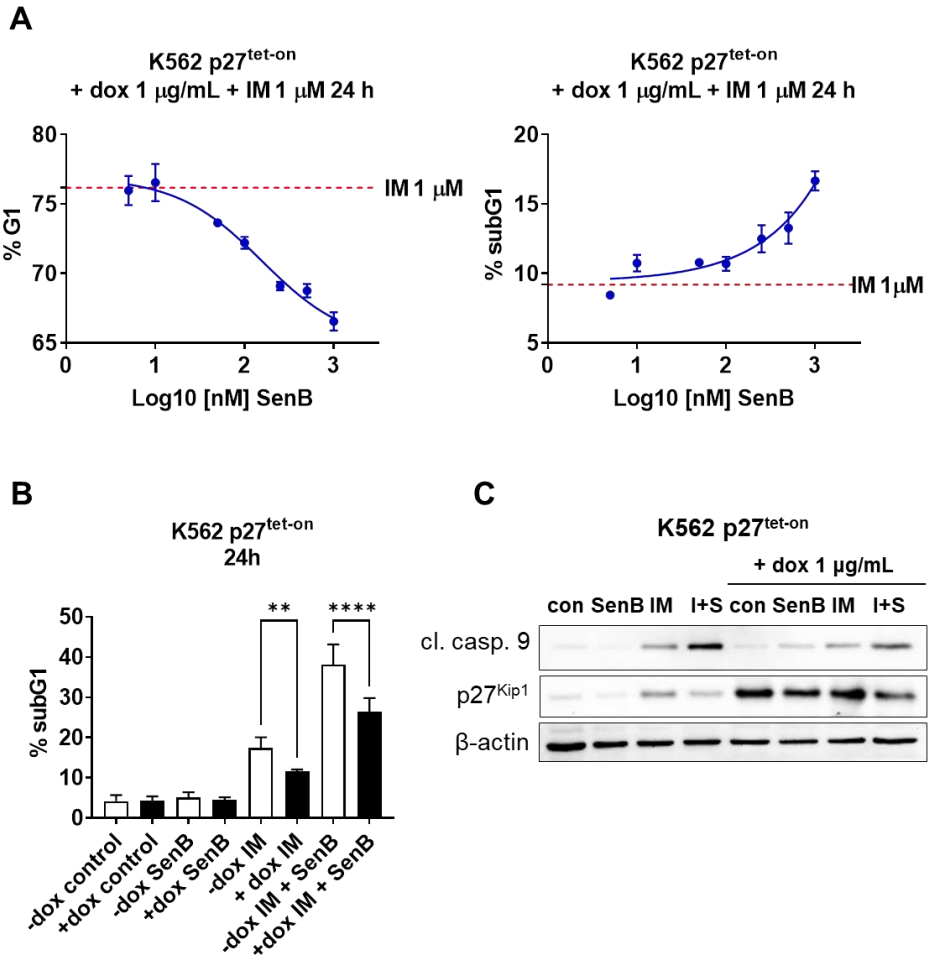

Figure 6. SenB counteracts the effects of exogenous *CDKN1B* (p27^{Kip1}) overexpression on cell cycle and survival.

K562p27tet-on subline was treated with 1 μg/ml doxycycline and 1 μM IM for 24 h in the absence or presence of indicated concentrations of SenB followed by flow cytometry analysis. (**A**) Decreased G1 arrest (*left*) and increased apoptotic DNA fragmentation (subG1; *right*). (**B**) SenB (1 μM) alleviates the protective effect of doxycycline on IM-induced apoptosis. (**C**) Exogenous p27^{Kip1} overexpression decreases apoptosis after treatment with SenB and IM (1 μM each) or the combination. **p<0.01, ****p<0.0001.

bioRxiv preprint doi: https://doi.org/10.1101/2023.09.25.559286; this version posted September 25, 2023. The copyright holder for this preprint (which was not certified by peer review) is the author/funder, who has granted bioRxiv a license to display the preprint in perpetuity. It is made available under aCC-BY-ND 4.0 International license.

Discussion

Treatment of CML with BCR-ABLi remains one of the most efficient anticancer therapy to date. Despite its success, patients must continue treatment to avoid relapse, due to persistence of resistant LSC (49) and/or emergence of de novo resistance. While *BCR-ABL* mutants are successfully treated with new generations of target inhibitors, non-mutational resistance remains challenging.

The Mediator protein kinases CDK8/19, in concert with a number of critical transcription factors, regulate effects of a variety of exogenous stimuli. CDK8/19 also directly phosphorylate transcription factors, such as STATs (50). CDK8/19 have been established as druggable antitumor targets, either alone (NCT04021368) or in combination with conventional therapeutics (29,30). Exploring the possibility to improve the efficacy of BCR-ABLi in CML cells, we herein demonstrated that SenB as well as other CDK8/19i sensitized the K562 CML cells to various BCR-ABLi (Figures 2A-D). The most significant effect of this sensitization was the increase in mitochondrial apoptosis (Figure 1). It was previously reported that CDK8 is downregulated by dasatinib but not by IM, and that siRNA knockdown of *CDK8* sensitizes cells to IM but not to dasatinib in K562 cells (51). In the present study, we have observed no changes of CDK8 expression by IM treatment upon 24 h exposure (Supplementary Figure S9), and CDK8/19i sensitized K562 to all BCR-ABL antagonists, including dasatinib (Figure 2). Possible causes for the different results obtained with *CDK8* siRNA and CDK8/19i are the effect of the inhibitors on CDK19 and the fact that *CDK8/19* depletion but not kinase inhibition leads to the degradation of cyclin C, which has CDK8/19 independent activities (23).

Activation of pro-survival pathways contributes to tumor cell persistence. Importantly, in at least 25% of cases and up to 60% of the resistance to BCR-ABLi stems from mechanisms independent of the structure of the *BCR-ABL* indicating non-genetic resistance (52). The major pro-survival pathways activated in response to BCR-ABL inhibition are STAT3 and STAT1 (53). In turn, inhibition of these pathways can increase the potency of BCR-ABLi. We found that the combination of SenB and IM reduced the amounts of total STAT1 and STAT3 phosphorylated at S727 (Figures 2B, 2D-E). Although S727 phosphorylation of STAT1/3 is considered as a marker for CDK8/19 activity (50), there is evidence that other kinases can phosphorylate it (43), so only partial inhibition by SenB alone can be explained by activity of other kinases. JAK2/STAT3 is a major contributor to BCR-ABLi resistance, activated by autocrine signaling (6) and cytokines secreted by the bone marrow (5). Inhibition of STAT3 can overcome resistance to BCR-ABLi and induce synthetic lethality in STAT3-dependent CML (5), including LSC (54).

From the onset of the TKI era in CML treatment, it became clear that non-dividing cells are much less sensitive to these drugs compared to proliferating counterparts. Subpopulations of quiescent LSC survived the exposure to BCR-ABLi resulting in disease relapse (55). IM induced apoptosis primarily in S and G2/M phases (56), therefore investigational strategies focused on eliminating quiescent cells or inhibitor-induced G1 cell cycle arrest. Altered response of CML cells to IM via quiescence has been reported (55,57). Quiescence has been attributed to the delay of full clinical remission (10,57), and may mediate the relapse of CML patients (11).

Our principal mechanistic finding is the identification of IM-induced G1 cell cycle arrest, mediated by $p27^{Kip1}$, as the critical mediator of the sensitization of CML cells to IM by CDK8/19 inhibition. IM treatment of K562 cells led to G1 accumulation (Figure 5A, *top left*) and upregulation of $p27^{Kip1}$ and $p18^{INK4c}$ (Figures 4B-C). Of note, $p27^{Kip1}$ and $p57^{Kip2}$ are inducible within the initial hours of treatment with IM (18). Furthermore, CKIs have been mechanistically related to LSC persistence (13,58). Strikingly, combining IM with a CDK8/19i released the cells from G1 arrest, elevated the fraction of cells entering

bioRxiv preprint doi: https://doi.org/10.1101/2023.09.25.559286; this version posted September 25, 2023. The copyright holder for this preprint (which was not certified by peer review) is the author/funder, who has granted bioRxiv a license to display the preprint in perpetuity. It is made available under aCC-BY-ND 4.0 International license.

replication (Figure 5B), and prevented the upregulation of $p27^{Kip1}$ (Figures 4A-B). Supporting the role of cell cycle regulation in the sensitivity to IM, in BCR-ABL positive KU812 cells IM influenced neither cell cycle progression nor CKI protein expression (Figures 4C, *right*, 5A, *right*). Rather, these cells readily underwent IM-induced death in a SenB independent manner.

The role of $p27^{Kip1}$ was confirmed by the results that inducible $p27^{Kip1}$ expression in K562 cells increased the G1 fraction and attenuated IM-induced apoptosis. Both of these effects were reversed by combining IM with SenB (Figure 6). Importantly, SenB alone counteracted $p27^{Kip1}$-induced G1 arrest, but evoked no significant effect on viability. These results show that CDK8/19i affects not only transcription, but also the activity of $p27^{Kip1}$. Similarly to our results, a CDK8/19i decreased $p27^{Kip1}$ RNA and protein levels and induced G1 to S transition in prostate cancer cells (59). On the other hand, CDK8 can act as a negative regulator of $p27^{Kip1}$ protein stability but does not affect its mRNA level in breast cancer cells (60); the different results that we obtained in CML cells suggest that the effect of CDK8 on $p27^{Kip1}$ is cell type-specific.

Altogether, we demonstrated that pharmacological inhibition of CDK8/19 promotes apoptosis in CML cells treated with BCR-ABLi by suppressing G1 arrest induced by these inhibitors. The mechanism is attributed to the effects of CDK8/19i on the $p27^{Kip1}$, which is upregulated by BCR-ABL inhibitors. Given that CDK8/19i evoke a negligible general toxicity (NCT03065010, NCT04021368, NCT05052255, NCT05300438), our results support the perspective of targeting these transcriptional kinases in situations when the efficacy of conventional drugs is limited.

bioRxiv preprint doi: https://doi.org/10.1101/2023.09.25.559286; this version posted September 25, 2023. The copyright holder for this preprint (which was not certified by peer review) is the author/funder, who has granted bioRxiv a license to display the preprint in perpetuity. It is made available under aCC-BY-ND 4.0 International license.

Materials and Methods

Reagents

All reagents were from Sigma-Aldrich, Burlington, MA, unless specified otherwise. IM (Gleevec®) was purchased from Novartis, Basel, Switzerland. Dasatinib and nilotinib were from Selleck Chemicals, Houston, TX. PF-114 (31) was a gift of Dr. G. Chilov. CDK8/19 inhibitors Senexin B (SenB) and SNX631/15U are from Senex Biotechnology, Columbia, SC.

Cell lines and culture conditions

Human CML cell lines K562 (Russian Collection of Cell Cultures, Saint-Petersburg, Russia) and KU812 (CRL-2099-ATCC, Manassas, VA) were propagated in RPMI-1640 (PanEco, Moscow, Russia) with 10% fetal bovine serum (Biosera, France), 2 mM *L*-glutamine, 100 U/ml penicillin and 100 µg/ml streptomycin (PanEco) at 37°C, 5% CO_2 in humidified atmosphere. Cells in the logarithmic phase of growth were used in the experiments.

Flow cytometry

Cell cycle distribution was analyzed as described (32). Cells were lysed in a buffer containing 50 µg/ml propidium iodide (PI), 100 µg/ml RNAse A, 0.1% sodium citrate, 0.3% NP-40 (VWR Life Science, Radnor, PA) for 30 min in the dark. Apoptosis was analyzed with eBioscience Annexin V Apoptosis Detection Kit APC (Thermo FS, Waltham, MA) in accordance with the manufacturer's recommendations. The MitoTracker® Red CMXRos (Invitrogen, Carlsbad, CA) was used to evaluate the mitochondrial membrane potential. Live/dead cells were determined by PI Nucleic Acid Stain (Thermo FS). Survival fraction was calculated as the percentage of PI negative cells after normalizing to the total cell count.

To assess cell proliferation, cells were labeled with 30 µg/ml 5-bromo-2'-deoxyuridine (BrdU) for 30 min, fixed with 70% ice cold ethanol for 5 min and treated with 1.5 M HCl for 30 min. Cells were stained with anti-BrdU antibody (Bu20a; BioRad, Hercules, CA) and counterstained with secondary Alexa Fluor® 488 conjugated antibody (Cell Signaling Technology, Danvers, MA), 50 µg/ml PI and 100 ug/ml RNAse A in saline. Fluorescence was measured on a Cytoflex flow cytometer 26 (Beckman Coulter, Indianapolis, IN). At least 10,000 events were collected per each sample, and analyzed using CytExpert Software (Beckman Coulter).

RNA sequencing (RNASeq)

Preparation of cDNA libraries

K562 cells (200×10^5 cells/ml) were treated with the vehicle (0.02% DMSO), 1 µM IM, 1 µM SenB or their combination (two replicates per each treatment) for 8 h. Total RNA was extracted with TRI reagent. 4 µg RNA was used to isolate poly(A)-enriched RNA with NEBNext® Poly(A) mRNA Magnetic Isolation Module (NE Biolabs, Ipswich, MA) that was used to prepare RNA sequencing libraries with NEBNext® Ultra™ II Directional RNA Library Prep Kit for Illumina (NE Biolabs). Actinomycin D was used for first strand cDNA synthesis; cDNA libraries ligated with the Illumina suitable adaptor sequences were generated and amplified with Q5 DNA polymerase (NE Biolabs). After purification from dimers by size selection in the agarose gel the libraries were sequenced on a NovaSeq 6000 (Illumina, San Diego, CA).

bioRxiv preprint doi: https://doi.org/10.1101/2023.09.25.559286; this version posted September 25, 2023. The copyright holder for this preprint (which was not certified by peer review) is the author/funder, who has granted bioRxiv a license to display the preprint in perpetuity. It is made available under aCC-BY-ND 4.0 International license.

Analysis of RNASeq data

Quality of short reads was checked using the FastQC software (33). Sequencing adaptors were removed using cutadapt (34), read ends with quality scores < 20 were trimmed and subsequently reads shorter than 30 bp were removed using sickle (35). Mapping of trimmed reads to human genome assembly GRCh37 (hg19) and calculation of per-gene read counts were performed using STAR (36).

Statistical analysis was conducted using the edgeR package (37). Only the genes with counts greater than one per million library reads (cpm>1) in at least two replicate samples were included. Read counts were normalized using the trimmed mean of values method implemented in edgeR. General linear models and the likelihood ratio test were used to identify differentially expressed genes (DEG). The Benjamini-Hochberg false discovery rate (FDR) correction was applied to the test results (alpha=0.05).

Over-representation analysis (ORA) using both Gene Ontology (GO) enrichment analysis of DEG and Reactome Pathways Database were conducted using the WebGestaltR package (38). The gene set enrichment analysis (GSEA) for different comparisons (39) was conducted using the fgsea package(40) with the specific gene sets downloaded from the Human Molecular Signatures Database (MSigDB). The ggplot2 (41) and clusterProfiler (42) R libraries were used for data visualization.

All raw RNA-Seq data were deposited in the Sequence Read Archive (SRA) under the BioProject accession PRJNA1008677 (to be released at the manuscript publication). Detailed information about RNA-Seq samples is listed in Table S4.

Lentiviral transduction

To obtain pCW-p27 lentiviral plasmid carrying $p27^{Kip1}$ ORF (RefSeq NM_004064.5), total RNA was isolated from IM-treated K562 cells. Complementary DNA was synthesized. Primers CDKN1B-forv 5'-attagctagcATGTCAAACGTGCGAGTGTCTAA-3' and CDKN1B-rev 5'-taatggatccTTACGTTTGACGTCTTCTGAGGC-3' (Evrogen, Moscow, Russia) containing NheI and BamHI restriction sites were used for amplification. The ORF was then cloned into the pCW vector replacing Cas9 in the pCW-Cas9 plasmid (https://www.addgene.org/50661/). The K562p27tet-on subline with doxycycline inducible $p27^{Kip1}$ overexpression was obtained by lentiviral transduction. The virus was concentrated by ultracentrifugation (120,000g) for 2 h at 4°C. Polybrene (20 µg/ml) was added, and the supernatant was mixed with K562 cells in the fresh medium (1:1 v/v). Selection was performed with 2 µg/ml puromycin. Exogenous $p27^{Kip1}$ was induced by 1 µg/ml doxycycline.

Immunoblotting

K562 and KU812 cells (200×10^5 cells/ml) were treated with 0.02% DMSO or drugs, harvested and lysed for 30 min on ice in a buffer containing 50 mM Tris-HCl pH 8.0, 150 mM NaCl, 0.1% sodium dodecyl sulfate, 1% NP-40, 2 mM phenylmethylsulfonyl fluoride (VWR Life Science, Radnor, PA) and the protease inhibitor cocktail. Protein concentrations were determined by the Bradford method. Lysates were separated by SDS-PAGE (30-50 µg total protein per lane) and transferred onto a 0.2 µm nitrocellulose membrane (Bio-Rad). Membranes were blocked with 5% skimmed milk for 30 min at RT and treated with primary antibodies (Supplementary Table S1) diluted in Tris-borate saline with Tween 20 (TBST) and 1% bovine serum albumin overnight at 4°C. Then membranes were washed with TBST and incubated with a secondary antibody conjugated with horseradish peroxidase for 1 h at RT. Proteins were visualized with the Clarity Western ECL Substrate (Bio-Rad) using the iBright FL1500 Imaging System (Invitrogen, Waltham, MA).

bioRxiv preprint doi: https://doi.org/10.1101/2023.09.25.559286; this version posted September 25, 2023. The copyright holder for this preprint (which was not certified by peer review) is the author/funder, who has granted bioRxiv a license to display the preprint in perpetuity. It is made available under aCC-BY-ND 4.0 International license.

Statistical analysis

The data are representative of at least three independent experiments. One-way or two-way analysis of variance (ANOVA) followed by Sidak's post hoc test for multiple comparisons was used (GraphPad Prism 9; GraphPad Software, San Diego, CA). P value <0.05 was taken as evidence of statistical significance.

Author Contributions

AIK, MAY, and VVT conceived and conducted the study, performed experiments, analyzed data, prepared the figures and graphs, and wrote the original draft. AVB and MAZ obtained the K562p27$^{tet\text{-}on}$ subline. C-UL, ESI, and JVN performed additional flow cytometry experiments. NEV prepared cDNA libraries for RNA-Seq, AMK, EAV, AVT, and JL analyzed the RNA-Seq data. ESI and YEA performed additional immunoblots. IBR, EVB, MC, and AAS discussed the project, reviewed and edited the manuscript. The text was read and approved by all authors.

Conflict of Interest

IBR is Founder and President and EVB and MC are consultants of Senex Biotechnology, Inc. Other authors declare no conflict of interest.

Acknowledgements

We thank the Center for Precision Genome Editing and Genetic Technologies for Biomedicine, Institute of Gene Biology, Russian Academy of Sciences, for supporting the research facilities. Studies conducted at the University of South Carolina in 2019-2021 were supported by the Microscopy and Flow Cytometry Core (MFCC) of the Center for Targeted Therapeutics.

Funding

This work was supported by Megagrant (Agreement №14.W03.31.0020 between the Ministry of Science and Education of the Russian Federation and Institute of Gene Biology, Russian Academy of Sciences). MFCC was supported by NIH COBRE grant P20 GM109091.

bioRxiv preprint doi: https://doi.org/10.1101/2023.09.25.559286; this version posted September 25, 2023. The copyright holder for this preprint (which was not certified by peer review) is the author/funder, who has granted bioRxiv a license to display the preprint in perpetuity. It is made available under aCC-BY-ND 4.0 International license.

References

1. Kang ZJ, Liu YF, Xu LZ, Long ZJ, Huang D, Yang Y, et al. The Philadelphia chromosome in leukemogenesis. Chin J Cancer. 2016 May 27;35:48.

2. Jabbour E, Kantarjian H. Chronic myeloid leukemia: 2020 update on diagnosis, therapy and monitoring. Am J Hematol. 2020 Jun;95(6):691–709.

3. Braun TP, Eide CA, Druker BJ. Response and Resistance to BCR-ABL1-Targeted Therapies. Cancer Cell. 2020 Apr 13;37(4):530–42.

4. Cortes J, Lang F. Third-line therapy for chronic myeloid leukemia: current status and future directions. J Hematol Oncol. 2021 Mar 18;14(1):44.

5. Bewry NN, Nair RR, Emmons MF, Boulware D, Pinilla-Ibarz J, Hazlehurst LA. Stat3 contributes to resistance toward BCR-ABL inhibitors in a bone marrow microenvironment model of drug resistance. Mol Cancer Ther. 2008 Oct;7(10):3169–75.

6. Eiring AM, Page BDG, Kraft IL, Mason CC, Vellore NA, Resetca D, et al. Combined STAT3 and BCR-ABL1 inhibition induces synthetic lethality in therapy-resistant chronic myeloid leukemia. Leukemia. 2015 Mar;29(3):586–97.

7. Ma L, Shan Y, Bai R, Xue L, Eide CA, Ou J, et al. A therapeutically targetable mechanism of BCR-ABL-independent imatinib resistance in chronic myeloid leukemia. Sci Transl Med. 2014 Sep 3;6(252):252ra121.

8. Neviani P, Harb JG, Oaks JJ, Santhanam R, Walker CJ, Ellis JJ, et al. PP2A-activating drugs selectively eradicate TKI-resistant chronic myeloid leukemic stem cells. J Clin Invest. 2013 Oct;123(10):4144–57.

9. Corbin AS, Agarwal A, Loriaux M, Cortes J, Deininger MW, Druker BJ. Human chronic myeloid leukemia stem cells are insensitive to imatinib despite inhibition of BCR-ABL activity. J Clin Invest. 2011 Jan;121(1):396–409.

10. Copland M, Hamilton A, Elrick LJ, Baird JW, Allan EK, Jordanides N, et al. Dasatinib (BMS-354825) targets an earlier progenitor population than imatinib in primary CML but does not eliminate the quiescent fraction. Blood. 2006 Jun 1;107(11):4532–9.

11. Graham SM, Vass JK, Holyoake TL, Graham GJ. Transcriptional analysis of quiescent and proliferating CD34+ human hemopoietic cells from normal and chronic myeloid leukemia sources. Stem Cells. 2007 Dec;25(12):3111–20.

12. Besson A, Gurian-West M, Chen X, Kelly-Spratt KS, Kemp CJ, Roberts JM. A pathway in quiescent cells that controls p27Kip1 stability, subcellular localization, and tumor suppression. Genes Dev. 2006 Jan 1;20(1):47–64.

13. Moreno-Lorenzana D, Avilés-Vazquez S, Sandoval Esquivel MA, Alvarado-Moreno A, Ortiz-Navarrete V, Torres-Martínez H, et al. CDKIs p18(INK4c) and p57(Kip2) are involved in quiescence

bioRxiv preprint doi: https://doi.org/10.1101/2023.09.25.559286; this version posted September 25, 2023. The copyright holder for this preprint (which was not certified by peer review) is the author/funder, who has granted bioRxiv a license to display the preprint in perpetuity. It is made available under aCC-BY-ND 4.0 International license.

of CML leukemic stem cells after treatment with TKI. Cell Cycle. 2016 May 2;15(9):1276–87.

14. Gesbert F, Sellers WR, Signoretti S, Loda M, Griffin JD. BCR/ABL regulates expression of the cyclin-dependent kinase inhibitor p27Kip1 through the phosphatidylinositol 3-Kinase/AKT pathway. J Biol Chem. 2000 Dec 15;275(50):39223–30.

15. Jonuleit T, van der Kuip H, Miething C, Michels H, Hallek M, Duyster J, et al. Bcr-Abl kinase down-regulates cyclin-dependent kinase inhibitor p27 in human and murine cell lines. Blood. 2000 Sep 1;96(5):1933–9.

16. Andreu EJ, Lledó E, Poch E, Ivorra C, Albero MP, Martínez-Climent JA, et al. BCR-ABL induces the expression of Skp2 through the PI3K pathway to promote p27Kip1 degradation and proliferation of chronic myelogenous leukemia cells. Cancer Res. 2005 Apr 15;65(8):3264–72.

17. Agarwal A, Mackenzie RJ, Besson A, Jeng S, Carey A, LaTocha DH, et al. BCR-ABL1 promotes leukemia by converting p27 into a cytoplasmic oncoprotein. Blood. 2014 Nov 20;124(22):3260–73.

18. Borriello A, Caldarelli I, Bencivenga D, Cucciolla V, Oliva A, Usala E, et al. p57Kip2 is a downstream effector of BCR-ABL kinase inhibitors in chronic myelogenous leukemia cells. Carcinogenesis. 2011 Jan;32(1):10–8.

19. Lee SH, Reed-Newman T, Anant S, Ramasamy TS. Regulatory Role of Quiescence in the Biological Function of Cancer Stem Cells. Stem Cell Rev Rep. 2020 Dec;16(6):1185–207.

20. Fant CB, Taatjes DJ. Regulatory functions of the Mediator kinases CDK8 and CDK19. Transcription. 2019 Apr;10(2):76–90.

21. Luyties O, Taatjes DJ. The Mediator kinase module: an interface between cell signaling and transcription. Trends Biochem Sci. 2022 Apr;47(4):314–27.

22. Pelish HE, Liau BB, Nitulescu II, Tangpeerachaikul A, Poss ZC, Da Silva DH, et al. Mediator kinase inhibition further activates super-enhancer-associated genes in AML. Nature. 2015 Oct 8;526(7572):273–6.

23. Chen M, Li J, Zhang L, Wang L, Cheng C, Ji H, et al. CDK8 and CDK19: positive regulators of signal-induced transcription and negative regulators of Mediator complex proteins. Nucleic Acids Res. 2023 Aug 11;51(14):7288–313.

24. Steinparzer I, Sedlyarov V, Rubin JD, Eislmayr K, Galbraith MD, Levandowski CB, et al. Transcriptional Responses to IFN-γ Require Mediator Kinase-Dependent Pause Release and Mechanistically Distinct CDK8 and CDK19 Functions. Mol Cell. 2019 Nov 7;76(3):485–99.e8.

25. Chen M, Liang J, Ji H, Yang Z, Altilia S, Hu B, et al. CDK8/19 Mediator kinases potentiate induction of transcription by NFκB. Proc Natl Acad Sci U S A. 2017 Sep 19;114(38):10208–13.

26. Westerling T, Kuuluvainen E, Mäkelä TP. Cdk8 is essential for preimplantation mouse development. Mol Cell Biol. 2007 Sep;27(17):6177–82.

bioRxiv preprint doi: https://doi.org/10.1101/2023.09.25.559286; this version posted September 25, 2023. The copyright holder for this preprint (which was not certified by peer review) is the author/funder, who has granted bioRxiv a license to display the preprint in perpetuity. It is made available under aCC-BY-ND 4.0 International license.

27. McCleland ML, Soukup TM, Liu SD, Esensten JH, de Sousa e Melo F, Yaylaoglu M, et al. Cdk8 deletion in the Apc(Min) murine tumour model represses EZH2 activity and accelerates tumourigenesis. J Pathol. 2015 Dec;237(4):508–19.

28. McDermott MSJ, Chumanevich AA, Lim CU, Liang J, Chen M, Altilia S, et al. Inhibition of CDK8 mediator kinase suppresses estrogen dependent transcription and the growth of estrogen receptor positive breast cancer. Oncotarget. 2017 Feb 21;8(8):12558–75.

29. Sharko AC, Lim CU, McDermott MSJ, Hennes C, Philavong KP, Aiken T, et al. The Inhibition of CDK8/19 Mediator Kinases Prevents the Development of Resistance to EGFR-Targeting Drugs. Cells [Internet]. 2021 Jan 12;10(1). Available from: http://dx.doi.org/10.3390/cells10010144

30. Ding X, Sharko AC, McDermott MSJ, Schools GP, Chumanevich A, Ji H, et al. Inhibition of CDK8/19 Mediator kinase potentiates HER2-targeting drugs and bypasses resistance to these agents in vitro and in vivo. Proc Natl Acad Sci U S A. 2022 Aug 9;119(32):e2201073119.

31. Mian AA, Rafiei A, Haberbosch I, Zeifman A, Titov I, Stroylov V, et al. PF-114, a potent and selective inhibitor of native and mutated BCR/ABL is active against Philadelphia chromosome-positive (Ph+) leukemias harboring the T315I mutation. Leukemia. 2015 May;29(5):1104–14.

32. Ivanova ES, Tatarskiy VV, Yastrebova MA, Khamidullina AI, Shunaev AV, Kalinina AA, et al. PF-114, a novel selective inhibitor of BCR-ABL tyrosine kinase, is a potent inducer of apoptosis in chronic myelogenous leukemia cells. Int J Oncol. 2019 Jul;55(1):289–97.

33. Andrews S. 2010. FastQC: a quality control tool for high throughput sequence data. Available online at: http://www.bioinformatics.babraham.ac.uk/projects/fastqc.

34. Martin M. Cutadapt removes adapter sequences from high-throughput sequencing reads. EMBnet.journal. 2011 May 2;17(1):10–2.

35. Joshi N.A., Fass J.N. 2011. Sickle: A sliding-window, adaptive, quality-based trimming tool for FastQ files (Version 1.33) [Software]. Available online at: https://github.com/najoshi/sickle.

36. Dobin A, Davis CA, Schlesinger F, Drenkow J, Zaleski C, Jha S, et al. STAR: ultrafast universal RNA-seq aligner. Bioinformatics. 2013 Jan 1;29(1):15–21.

37. Robinson MD, McCarthy DJ, Smyth GK. edgeR: a Bioconductor package for differential expression analysis of digital gene expression data. Bioinformatics. 2010 Jan 1;26(1):139–40.

38. Liao Y, Wang J, Jaehnig EJ, Shi Z, Zhang B. WebGestalt 2019: gene set analysis toolkit with revamped UIs and APIs. Nucleic Acids Res. 2019 Jul 2;47(W1):W199–205.

39. Subramanian A, Tamayo P, Mootha VK, Mukherjee S, Ebert BL, Gillette MA, et al. Gene set enrichment analysis: a knowledge-based approach for interpreting genome-wide expression profiles. Proc Natl Acad Sci U S A. 2005 Oct 25;102(43):15545–50.

40. Korotkevich G, Sukhov V, Budin N, Shpak B, Artyomov MN, Sergushichev A. Fast gene set enrichment analysis [Internet]. bioRxiv. 2021 [cited 2023 Sep 13]. p. 060012. Available from:

bioRxiv preprint doi: https://doi.org/10.1101/2023.09.25.559286; this version posted September 25, 2023. The copyright holder for this preprint (which was not certified by peer review) is the author/funder, who has granted bioRxiv a license to display the preprint in perpetuity. It is made available under aCC-BY-ND 4.0 International license.

https://www.biorxiv.org/content/10.1101/060012v3

41. Wickham H. 2016. ggplot2: Elegant Graphics for Data Analysis. Springer-Verlag New York. ISBN 978-3-319-24277-4, https://ggplot2.tidyverse.org.

42. Wu T, Hu E, Xu S, Chen M, Guo P, Dai Z, et al. clusterProfiler 4.0: A universal enrichment tool for interpreting omics data. Innovation (Camb). 2021 Aug 28;2(3):100141.

43. Chen M, Li J, Liang J, Thompson ZS, Kathrein K, Broude EV, et al. Systemic Toxicity Reported for CDK8/19 Inhibitors CCT251921 and MSC2530818 Is Not Due to Target Inhibition. Cells [Internet]. 2019 Nov 9;8(11). Available from: http://dx.doi.org/10.3390/cells8111413

44. Li J, Ji H, Porter DC, Broude EV, Roninson IB, Chen M. Characterizing CDK8/19 Inhibitors through a NFκB-Dependent Cell-Based Assay. Cells [Internet]. 2019 Oct 6;8(10). Available from: http://dx.doi.org/10.3390/cells8101208

45. Coppo P, Flamant S, De Mas V, Jarrier P, Guillier M, Bonnet ML, et al. BCR-ABL activates STAT3 via JAK and MEK pathways in human cells. Br J Haematol. 2006 Jul;134(2):171–9.

46. Sayed D, Badrawy H, Gaber N, Khalaf MR. p-Stat3 and bcr/abl gene expression in chronic myeloid leukemia and their relation to imatinib therapy. Leuk Res. 2014 Feb;38(2):243–50.

47. Liu Y, Perdreau SA, Chatterjee P, Wang L, Kuan SF, Duensing A. Imatinib mesylate induces quiescence in gastrointestinal stromal tumor cells through the CDH1-SKP2-p27Kip1 signaling axis. Cancer Res. 2008 Nov 1;68(21):9015–23.

48. Gómez-Casares MT, García-Alegria E, López-Jorge CE, Ferrándiz N, Blanco R, Alvarez S, et al. MYC antagonizes the differentiation induced by imatinib in chronic myeloid leukemia cells through downregulation of p27(KIP1.). Oncogene. 2013 Apr 25;32(17):2239–46.

49. Chomel JC, Bonnet ML, Sorel N, Sloma I, Bennaceur-Griscelli A, Rea D, et al. Leukemic stem cell persistence in chronic myeloid leukemia patients in deep molecular response induced by tyrosine kinase inhibitors and the impact of therapy discontinuation. Oncotarget. 2016 Jun 7;7(23):35293–301.

50. Martinez-Fabregas J, Wang L, Pohler E, Cozzani A, Wilmes S, Kazemian M, et al. CDK8 Fine-Tunes IL-6 Transcriptional Activities by Limiting STAT3 Resident Time at the Gene Loci. Cell Rep. 2020 Dec 22;33(12):108545.

51. Nunoda K, Tauchi T, Takaku T, Okabe S, Akahane D, Sashida G, et al. Identification and functional signature of genes regulated by structurally different ABL kinase inhibitors. Oncogene. 2007 Jun 14;26(28):4179–88.

52. Zhao H, Deininger MW. Declaration of Bcr-Abl1 independence. Leukemia. 2020 Nov;34(11):2827–36.

53. Poudel G, Tolland MG, Hughes TP, Pagani IS. Mechanisms of Resistance and Implications for Treatment Strategies in Chronic Myeloid Leukaemia. Cancers [Internet]. 2022 Jul 6;14(14). Available from: http://dx.doi.org/10.3390/cancers14143300

bioRxiv preprint doi: https://doi.org/10.1101/2023.09.25.559286; this version posted September 25, 2023. The copyright holder for this preprint (which was not certified by peer review) is the author/funder, who has granted bioRxiv a license to display the preprint in perpetuity. It is made available under aCC-BY-ND 4.0 International license.

54. Kuepper MK, Bütow M, Herrmann O, Ziemons J, Chatain N, Maurer A, et al. Stem cell persistence in CML is mediated by extrinsically activated JAK1-STAT3 signaling. Leukemia. 2019 Aug;33(8):1964–77.

55. Warfvinge R, Geironson L, Sommarin MNE, Lang S, Karlsson C, Roschupkina T, et al. Single-cell molecular analysis defines therapy response and immunophenotype of stem cell subpopulations in CML. Blood. 2017 Apr 27;129(17):2384–94.

56. Jørgensen HG, Allan EK, Mountford JC, Richmond L, Harrison S, Elliott MA, et al. Enhanced CML stem cell elimination in vitro by bryostatin priming with imatinib mesylate. Exp Hematol. 2005 Oct;33(10):1140–6.

57. Graham SM, Jørgensen HG, Allan E, Pearson C, Alcorn MJ, Richmond L, et al. Primitive, quiescent, Philadelphia-positive stem cells from patients with chronic myeloid leukemia are insensitive to STI571 in vitro. Blood. 2002 Jan 1;99(1):319–25.

58. Chu S, McDonald T, Bhatia R. Role of BCR-ABL-Y177-mediated p27kip1 phosphorylation and cytoplasmic localization in enhanced proliferation of chronic myeloid leukemia progenitors. Leukemia. 2010 Apr;24(4):779–87.

59. Nakamura A, Nakata D, Kakoi Y, Kunitomo M, Murai S, Ebara S, et al. CDK8/19 inhibition induces premature G1/S transition and ATR-dependent cell death in prostate cancer cells. Oncotarget. 2018 Mar 2;9(17):13474–87.

60. Xu D, Li CF, Zhang X, Gong Z, Chan CH, Lee SW, et al. Skp2-macroH2A1-CDK8 axis orchestrates G2/M transition and tumorigenesis. Nat Commun. 2015 Mar 30;6:6641.